Role of Ligand Substitution in Ferrocytochrome *c* Folding†

Jason R. Telford, F. Akif Tezcan, Harry B. Gray,* and Jay R. Winkler*

Beckman Institute, California Institute of Technology, Pasadena, California 91125

Received August 11, 1998; Revised Manuscript Received October 21, 1998

ABSTRACT: The ligand substitutions that occur during the folding of ferrocytochrome *c* [Fe(II)cyt *c*] have been monitored by transient absorption spectroscopy. The folding reaction was triggered by photoinduced electron transfer to unfolded Fe(III)cyt *c* in guanidine hydrochloride (GuHCl) solutions. Assignments of ligation states were made by reference to the spectra of the imidazole and methionine adducts of *N*-acetylated microperoxidase 8. At pH 7, the heme in unfolded Fe(II)cyt *c* is ligated by native His18 and HisX (X = 26, 33) residues. The native Met80 ligand displaces HisX only in the last stages of folding. The ferroheme is predominantly five-coordinate in acidic solution; it remains five-coordinate until the native methionine binds the heme to give the folded protein (the rate of the methionine binding step is 16 ± 5 s^{-1} at pH 5, 3.2 M GuHCl). The evidence suggests that the substitution of histidine by methionine is strongly coupled to backbone folding.

The kinetics of folding cytochrome *c* (cyt *c*)[1] have been studied in many laboratories (*1*−*10*). The heme iron in the folded protein is coordinated to two axial ligands, an imidazole nitrogen from His18 and a thioether sulfur from Met80 (Figure 1) (*11*). When Fe(III)cyt *c* is denatured by guanidine hydrochloride (GuHCl) at neutral pH, far-UV circular dichroism (CD) measurements reveal a cooperative unfolding transition with a midpoint at 2.7 M GuHCl (*12, 13*). The CD spectra suggest that all secondary structure is lost above 3.5 M GuHCl (*12, 13*). Small-angle X-ray scattering measurements (SAXS) of the Fe(III)cyt *c* radius of gyration (R_g) also show a cooperative unfolding transition with a midpoint at 2.6 M GuHCl; the value of R_g increases from 13.8 ± 0.3 to 30.3 ± 0.1 Å as the protein unfolds (*14*). Kratky plots of the SAXS data were interpreted in terms of two ensembles of unfolded protein; the dominant ensemble at 2.8 M GuHCl is not globular but retains some residual structure. Above 3.5 M GuHCl, the SAXS data suggest that Fe(III)cyt *c* is a random coil (*14*). It is likely that there are many unfolded states of the protein; the two ensembles identified in the SAXS analysis represent averages corresponding to the different denaturing conditions (*14*). In addition to peptide conformational changes, GuHCl also induces replacement of the Met80 axial ligand by a histidine residue. In the equine protein, both His26 and His33 have been implicated as ligands in the unfolded protein, although recent work suggests that His33 dominates (*15*). Under more acidic denaturing conditions, one or both of the axial ligands can be replaced by water. It is clear, then, that cyt *c* folding requires not only the arrangement of a polypeptide into a discrete three-dimensional structure but also heme ligand substitution processes (*1, 3, 6, 7, 16*−*22*).

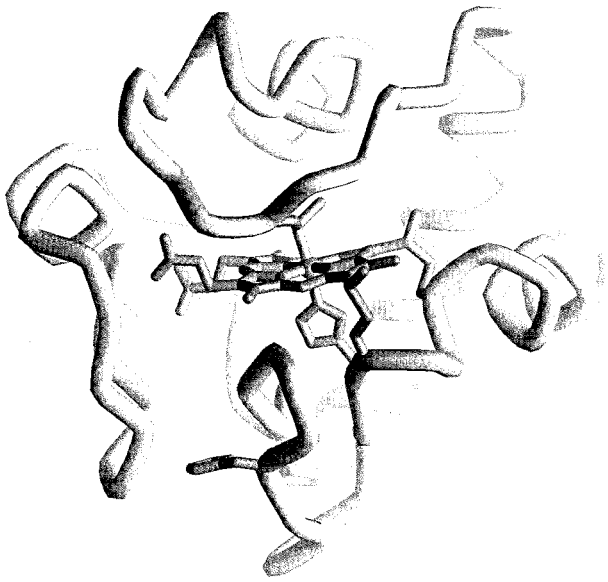

FIGURE 1: Backbone structure of horse heart cytochrome *c* (*11*). The axial ligands in the native protein are His18 and Met80; shown in the lower part of the structure are the side chains of the His*X* (*X* = 26, 33) residues that can ligate the heme iron in the unfolded protein.

The HisX (X = 26, 33) ligands present in unfolded Fe(III)cyt *c* at neutral pH lead to kinetic traps as the polypeptide tries to fold. Time-resolved resonance Raman studies suggest that HisX is not replaced directly by Met80; instead, formation of the folded protein involves an intermediate with His18/H_2O axial ligation (*7, 17, 21*). At neutral pH, it is generally agreed that the unfolded peptide collapses around the heme prior to the replacement of Met80 for HisX, but there is considerable disagreement about the time scale. At lower pH, where the HisX traps are not formed, there is debate about whether peptide folding and ligand substitution are sequential or concerted processes (*18, 19, 21, 23*).

† Supported by the National Science Foundation (MCB 9630465) and the National Institutes of Health (GM18660 to J.R.T.).

[1] Abbreviations: cyt *c*, cytochrome *c*; cyt$_u$ *c*, unfolded cytochrome *c*; cyt b_{562}, cytochrome b_{562}; GuHCl, guanidine hydrochloride; bpy, 2,2′-bipyridine; *Ru(bpy)$_3^{2+}$, electronically excited Ru(bpy)$_3^{2+}$; AcMP8, *N*-acetylated heme octapeptide (residues 14−21) from cytochrome *c*; CD, circular dichroism; SAXS, small-angle X-ray scattering; R_g, radius of gyration; ET, electron transfer.

10.1021/bi981933z CCC: $18.00
Published on Web 01/22/1999

There have been relatively few investigations of Fe(II)-cyt *c* folding. Given that metal−ligand binding constants and substitution rates are dependent on the metal oxidation state, it is possible that key steps in the folding of the reduced protein could differ markedly from those of Fe(III)cyt *c*. Indeed, in a study of folding initiated by photochemical dissociation of CO from the unfolded carbonmonoxy form of Fe(II)cyt *c*, a 40-μs time constant for Met80 binding was reported (*8*, *24*, *25*). This rate is about 100 times higher than that of Met80 binding during the folding of the oxidized protein at low pH (*26*).

We have shown previously that photoinduced electron injection into unfolded Fe(III)cyt *c* triggers the folding of the reduced protein (*4*, *9*, *10*). Electronically excited Ru(bpy)$_3^{2+}$ (bpy = 2,2′-bipyridine) is a powerful reductant, and its 600-ns lifetime makes it an excellent reagent for initiating folding on the microsecond time scale. We also have shown that NADH is a useful photoreductant (*27*−*29*): two-photon excitation (355 nm) of NADH produces a proton and two powerful reducing species, a solvated electron and NAD$^\bullet$ (*30*, *31*). Both reductants reduce unfolded Fe(III)cyt *c* (100 μM) in less than 100 μs.

We have employed transient absorption spectroscopy to probe the kinetics of the heme-ligand substitutions that accompany the folding of Fe(II)cyt *c* following photoinduced electron transfer (ET) to unfolded ferricytochrome *c*. We could not prepare at a suitable denaturant concentration all of the possible axial-ligand adducts of unfolded cyt *c*. Instead, we have used the *N*-acetylated heme octapeptide from cyt *c* (AcMP8), and its axial-ligand adducts, to model the spectra of possible transient intermediates formed during Fe(II)cyt *c* folding. Our results are consistent with a mechanism in which HisX ligation at neutral pH leads to a kinetic trap. The importance of this trap is diminished at low pH, where folding is limited by the rate of formation of the Fe−S(Met80) bond.

MATERIALS AND METHODS

Type VI horse heart cytochrome *c* (Sigma) was used without further purification. Guanidine hydrochloride (GuHCl) (U.S. Biochemical Corp., ultrapure grade) concentrations were determined by measuring the refractive index of the solution (*32*). Microperoxidase 8 (MP8), the heme octapeptide obtained by enzymatic digestion of horse cytochrome *c*, and N-terminal acetylated MP8 (AcMP8), which is less prone to aggregation, were prepared according to published procedures (*33*−*35*).

Steady-state absorption spectra were recorded with a Hewlett-Packard 8452 diode array spectrophotometer. Transient absorption kinetics and spectra were measured as previously described (*36*). Samples were excited with pulses from an excimer-pumped dye laser (480 nm, 1−4 mJ, 25 ns pulse) for experiments with Ru(bpy)$_3^{2+}$, or the third harmonic (355 nm, ≤ 10 mJ, 8 ns pulse) from a Q-switched Nd−YAG laser for experiments utilizing NADH as a photoreductant.

Samples for transient absorption kinetics were deoxygenated by repeated evacuation/argon-fill cycles on a Schlenk line. Protein concentrations were typically 100 μM. For measurements from 1 μs to 5 ms, Ru(bpy)$_3^{2+}$ (250 μM) was used as the photoreductant. For longer time scales (100 μs−1 s), NADH (100 μM) was used to deliver electrons. All samples were prepared in 50 mM sodium phosphate buffer (pH 7). The pH of each of the samples containing NADH was checked before and after laser experiments to ensure that no change occurred. If necessary, the pH was adjusted by addition of 0.1 M HCl or 0.1 M KOH. A stock solution ([Im] = 0.99 M) was used to prepare samples containing imidazole.

The pH-induced ligand dissociation of (HisX)(His18)Fe(III/II)cyt$_u$ *c* was monitored by changes in Soret absorbance. All titrations were performed at 22 ± 1 °C in degassed buffer solutions. The titration of Fe(III)cyt$_u$ *c* was performed in 50 mM phosphate buffer and 3.2 M GuHCl. The Fe(II)cyt$_u$ *c* titration was performed in 50 mM phosphate buffer and 5.5 M GuHCl in the presence of excess dithionite to ensure complete reduction of the protein. The change in intensity at 398 nm [Fe(III)cyt$_u$ *c*] or 524 nm [Fe(II)cyt$_u$ *c*] was plotted against pH to determine the pK_a of the histidine bound to the heme. The pH was adjusted by the addition of small volumes of 1.00 M NaOH or 1.00 M HCl to the denatured protein. The pH was measured with a calibrated microelectrode (Orion model 9826). pK_a values were obtained from pH titrations; no correction was applied for high [GuHCl]. The data were fit by nonlinear least-squares methods to:

$$\mathrm{Abs_{pH}} = \frac{\mathrm{Abs_{pH4.5}} + \mathrm{Abs_{pH7.5}} n(\mathrm{p}K_a - \mathrm{pH})}{1 + 10^{n(\mathrm{p}K_a - \mathrm{pH})}}$$

where n is the number of protons involved and pK_a is the midpoint of the transition.

RESULTS AND DISCUSSION

Spectra of Model Compounds: (Im)AcMP8 and (Met)-AcMP8. Absorption in the Soret region (375−450 nm) is a sensitive probe of the oxidation and spin states of the AcMP8 heme (Figure 2): (H_2O)(His18)Fe(III)AcMP8 is a mixed-spin, six-coordinate complex, with water or hydroxide occupying the sixth ligand site (λ_{max} = 396 nm); imidazole (Im) readily replaces the aquo ligand (log K= 4.5), generating low-spin (Im)(His18)Fe(III)AcMP8 (λ_{max} = 404 nm) (*37*). The spectrum of this adduct is nearly identical with that of unfolded ferricytochrome *c*, (HisX)(His18)Fe(III)cyt$_u$ *c*. Since the formation constant for the methionine adduct of Fe(III)-AcMP8 is quite small (log K = 0.4), only partial methionine binding is seen even at Met concentrations > 1 M (*38*). Hence, the spectrum of (Met)(His18)Fe(III)AcMP8 (λ_{max} = 410 nm) was determined from that of (H_2O)(His18)Fe(III)-AcMP8 in the presence of 2 M methionine (*38*).

The (His18)Fe(II)AcMP8 spectrum (λ_{max} = 409 nm) (pH 7) is similar to the spectrum of the Met80Ala mutant of Fe(II)cyt *c*, which has been interpreted in terms of an equilibrium mixture of high-spin/five-coordinate and low-spin/six-coordinate heme species (*39*, *40*). Resonance Raman spectra suggest that the dominant form of (His18)Fe(II)-AcMP8 is high-spin (*38*). Both (Im)(His18)Fe(II)AcMP8 (λ_{max} = 413 nm) and (Met)(His18)Fe(II)AcMP8 (λ_{max} = 416 nm) exhibit spectra characteristic of six-coordinate, low-spin ferrohemes.

pH Titrations of Unfolded Cyt c. In the unfolded protein at pH 7, the Met80 ligand is replaced by HisX (X = 26 or 33) (*15*). Absorption changes indicate that acidification of

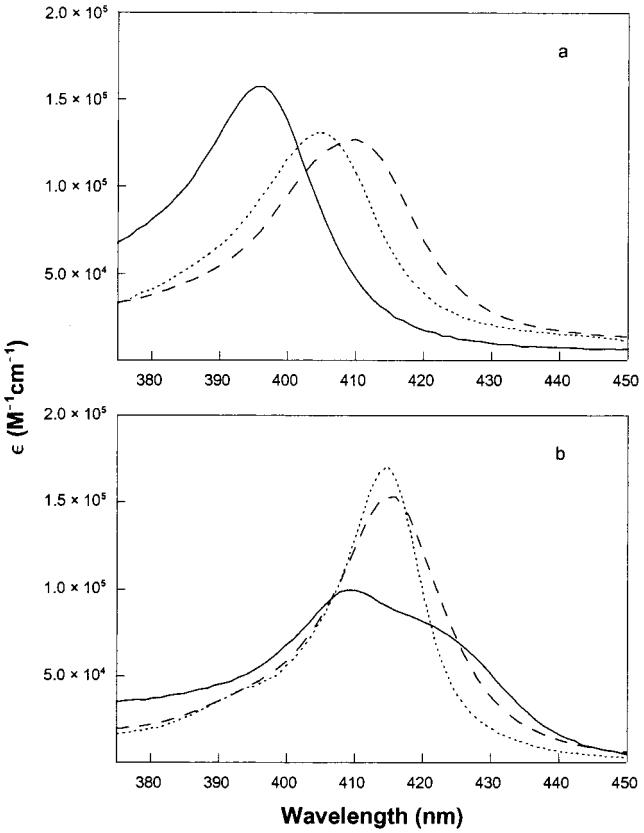

FIGURE 2: Spectra of (a) oxidized and (b) reduced AcMP8: no exogenous ligand (—); axial imidazole (···); axial methionine (– – –).

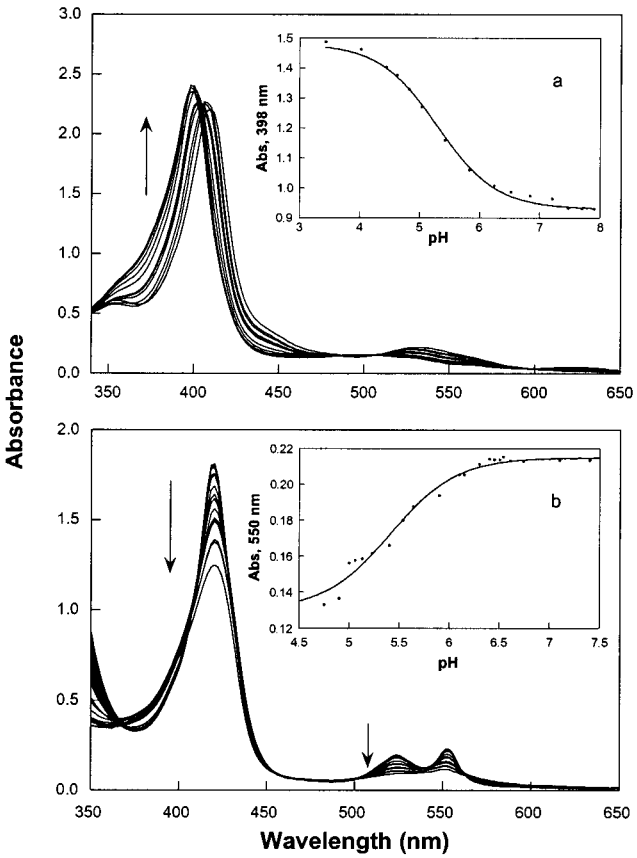

FIGURE 3: Changes in spectra observed during the pH titrations of unfolded (a) oxidized and (b) reduced cytochrome *c*. The insets show the absorbance vs pH data and the calculated curve for a single protonation step.

(HisX)(His18)Fe(III)cyt$_u$ *c* and (HisX)(His18)Fe(II)cyt$_u$ *c* solutions converts the heme from a low-spin state, consistent with two axial ligands, to a mixed-spin or high-spin species, indicating the loss of one of the histidines (Figure 3) (*1, 41*). The AcMP8 model spectra were used to assign the species present during the acid titrations. The misligated axial histidine is replaced by water in Fe(III)cyt$_u$ *c*; in contrast, the heme appears to remain five-coordinate after dissociation of the nonnative ligand in Fe(II)cyt$_u$ *c*.

The pK_a values for the protonation and dissociation of the nonnative axial histidine ligand are 5.3 ± 2 [Fe(III)cyt$_u$ *c*] and 5.5 ± 2 [Fe(II)cyt$_u$ *c*]. The titration curves for both oxidized and reduced forms of (HisX)(His18)Fe cyt$_u$ *c* are well described by a model involving a single protonation step. The higher pK_a for Fe(II)cyt$_u$ *c* indicates that the misligated histidine is bound less strongly to the reduced heme. Consistent with this observation is the −40-mV shift in the Fe(III/II) reduction potential upon binding imidazole to (H_2O)(His18)Fe(III)AcMP8 (*38*). Our results are in reasonable agreement with other values [pK_a = 5.7 (*15*) and 5.1 (*42*)] reported for the acid-induced transition of unfolded Fe(III)cyt *c*. The native histidine ligand, His18, is strongly bound to the heme [pK_a ~2.8 for Fe(III)cyt *c*; ~3.8 for Fe(II)cyt *c*] by virtue of its position in the polypeptide chain (adjacent to Cys17, which forms a thioether linkage with the porphyrin) (*43*).

Transient Spectra of AcMP8. In the ET-triggered experiments, the dominant form in the initial state is (HisX)(His18)-Fe(III)cyt$_u$ *c* at pH 7 or (H_2O)(His18)Fe(III)cyt$_u$ *c* at pH 4.5. To distinguish the changes in spectra associated with folding from those arising from the folding trigger, we have studied transient spectra of (H_2O)(His18)Fe(III)AcMP8 and (Im)-(His18)Fe(III)AcMP8 following photochemical reduction. Immediately after reduction by *Ru(bpy)$_3^{2+}$ (t > 5 μs), the transient spectrum of AcMP8 closely matches the steady-state (His18)Fe(II)AcMP8 spectrum, indicating that loss of the axial water ligand to give a five-coordinate, high-spin heme is relatively rapid. Photochemical reduction of (Im)-(His18)Fe(III)AcMP8 (pH 7) produces a six-coordinate, low-spin heme. The transient difference spectrum of this species can be reproduced by the steady-state difference spectrum of (Im)Fe(III/II)AcMP8 without any contribution from five-coordinate Fe(II)AcMP8. The only process observed after excited-state decay is the reoxidation of either (His18)Fe-(II)AcMP8 or (Im)(His18)Fe(II)AcMP8 by Ru(bpy)$_3^{3+}$.

Fe(II)cyt c Folding, pH 7. At neutral pH (3.2 M [GuHCl]), there is a rapid change in the heme absorbance following electron injection from *Ru(bpy)$_3^{2+}$ into (HisX)(His18)Fe-(III)cyt$_u$ *c*. The transient difference spectrum recorded 5 μs after the laser flash is essentially identical with the spectrum observed following reduction of (Im)(His18)Fe(III)AcMP8, suggesting formation of (HisX)(His18)Fe(II)cyt$_u$ *c* (Figure 4). The only discernible process in the microsecond to millisecond time range is the reoxidation of (HisX)(His18)-Fe(II)cyt$_u$ *c* by Ru(bpy)$_3^{3+}$; there is no evidence for ligand substitution during this time period.

We employed NADH as a photoreductant to study Fe-(II)cyt *c* folding between 100 μs and 1 s. Since the photolysis of NADH produces reducing equivalents and no other species (reoxidation of the protein does not occur), folding can be

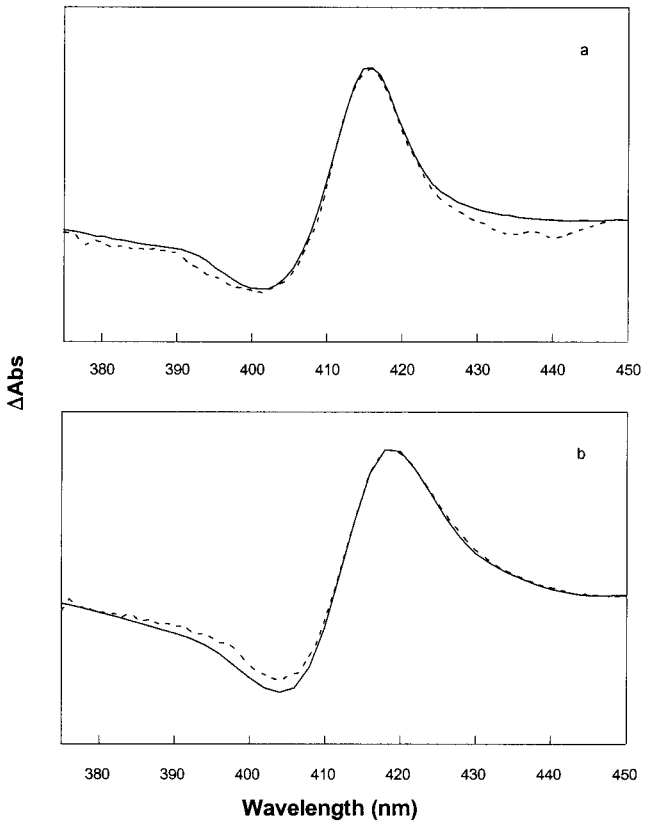

FIGURE 4: (a) Time-resolved difference spectrum of cyt *c* (3.2 M [GuHCl]) at 100 μs following reduction (···) is shown with the steady-state difference spectrum Fe(II) − Fe(III)(Im)(His18)AcMP8 (—). (b) Time-resolved difference spectrum of cyt *c* (3.2 M [GuHCl]) at 500 ms following NADH photoreduction (···) is shown with the steady-state difference spectrum Fe(II)cyt$_f$ *c* − Fe(III)cyt$_u$ *c* (—).

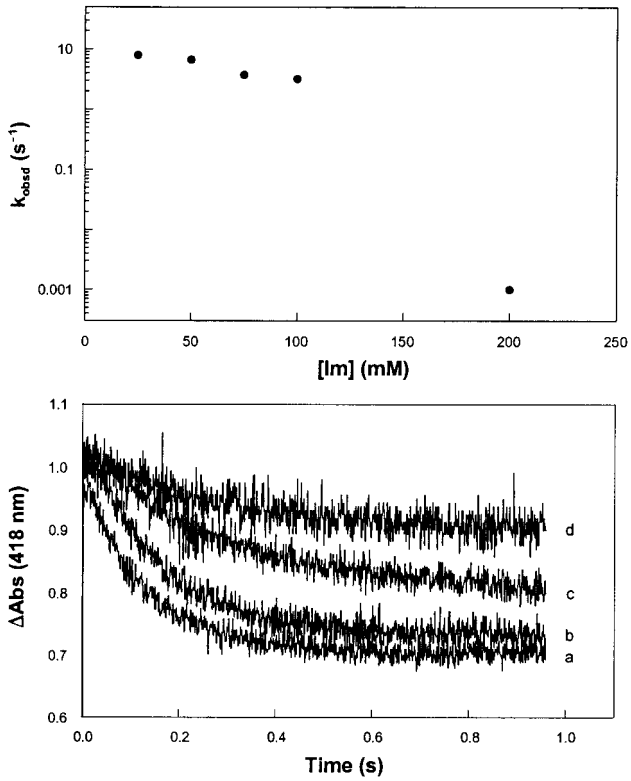

FIGURE 5: (Upper panel) Dependence of the (Met80)(His18)Fe(II)cyt *c* formation rate (k_{obsd}) on [Im] in 3.2 M GuHCl solution. (Lower panel) Kinetics traces (418 nm) at [Im] values of (a) 25 mM, (b) 50 mM, (c) 75 mM, and (d) 100 mM. As [Im] increases, both the rate of formation and yield of folded protein are diminished.

monitored on much longer time scales. Significant changes in Soret absorbance appear 50−100 ms after electron injection. By 400 ms following the laser flash, the transient difference spectrum of Fe(II)cyt *c* closely matches that expected for (Met80)(His18)Fe(II)cyt$_f$ *c*. Thus, the substitution reaction that restores the Met80 ligand to Fe(II)cyt *c* takes place in the 50−400 ms time interval. There is no indication that a high-spin (i.e., five-coodinate) intermediate is formed during the folding of Fe(II)cyt *c* at pH 7. Instead, the kinetics of Fe(II)cyt *c* folding (pH 7) are adequately modeled by a single-exponential phase and show a strong dependence on driving force.

Fe(II)cyt c Folding in the Presence of Imidazole, pH 7. The addition of a large excess of imidazole (>10 mM) converts (HisX)(His18)Fe(III)cyt$_u$ *c* to (Im)(His18)Fe(III)-cyt$_u$ *c* (*15*). Although the addition of imidazole increases the rate of folding of Fe(III)cytochrome *c* (*20*), it slows the binding of Met80 to the heme in the reduced protein.

The kinetics and Soret absorbance changes that accompany folding of Fe(II)cyt$_u$ *c* ([GuHCl] = 3.2 M) were monitored as a function of added imidazole (Figure 5). The rate of (Met80)(His18)Fe(II)cyt *c* formation decreases with increasing imidazole concentration; at very high [Im] (>100 mM), there is no sign of (Met80)(His18)Fe(II)cyt$_f$ *c*, even 5 s after electron injection. The data do not necessarily show that Fe(II)cyt *c* does not fold in the presence of imidazole. The major changes in the Soret absorbance report on the heme ligation state; the optical changes associated with polypeptide folding are likely to be small. In the presence of a large excess of imidazole, either the protein does not fold or it folds around the misligated heme. The latter explanation is plausible, since it is known that imidazole will bind to the folded oxidized protein, although some reorganization of the heme pocket is required (*44*).

Fe(II)cyt c Folding, pH < 5. At lower pH, nonnative histidine−heme ligation in unfolded Fe(III)cyt *c* is disfavored and the axial coordination sites are occupied by water and His18, giving rise to a mixed-spin ferric heme. Under these conditions, folding is markedly faster than at neutral pH and a single kinetics phase is observed in stopped-flow studies with Trp fluorescence or S(Met80)Fe(III) charge-transfer absorption as a probe (*20*, *22*).

In the unfolded oxidized and reduced proteins, the pK_a values of the two axial histidine ligands are so similar that there is no pH where His18 is bound but HisX is completely dissociated. Our studies of the ET-triggered folding kinetics of Fe(II)cyt$_u$ *c* cover the pH range 8.0−5.0, where His18 is bound, and the fraction of the population with HisX bound decreases from 100% to 33% (100% to 24%) for the oxidized (reduced) unfolded protein.

Distinct changes in the folding kinetics of Fe(II)cyt$_u$ *c* are seen at lower pH (Figure 6). Between pH 8 and 5.5, the kinetics of Fe(II)cyt$_f$ *c* formation are monoexponential, the rate increasing only slightly as the pH is lowered. Below pH 5.5, the kinetics are distinctly biphasic. The rate constant for the faster process is sensitive to pH, increasing by an order of magnitude as the pH is lowered from 5.5 to 4.5. The rate constant for the slower process is independent of pH, remaining constant within error at 16 ± 5 s^{-1}.

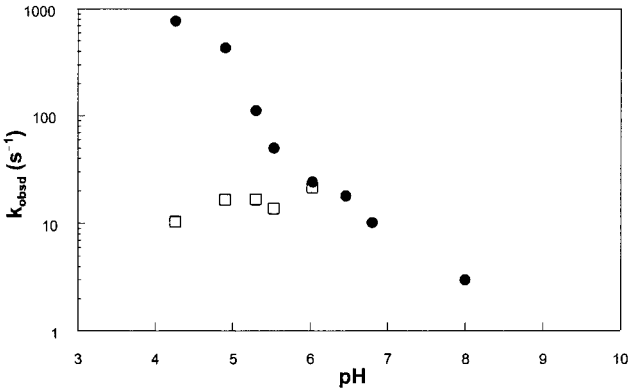

FIGURE 6: Dependence of rate constants on pH. Above pH 6, a single phase is observed (●); at lower pH values, kinetics are biexponential (●, fast phase; □, slow phase).

At pH 5, the oxidized unfolded protein is 67% mixed-spin (H_2O)(His18)Fe(III)cyt$_u$ *c* and 33% low-spin (HisX)-(His18)Fe(III)cyt$_u$ *c*. The reduced unfolded protein, with an apparent pK_a ~ 5.5, has an equilibrium population of 24% (HisX)(His18)Fe(II)cyt$_u$ *c* at pH 5. The fast process observed below pH 5.5 can be attributed to the approach to the equilibrium ligation state of the reduced heme. The transient spectrum measured 1 ms after reduction (pH 5.0) can be modeled by two absorbing heme species, with the majority fraction (65%) being a high-spin ferroheme. On the basis of its similarity to the spectrum of (His18)Fe(II)AcMP8, this intermediate is assigned as a five-coordinate heme. The minority fraction is attributed to six-coordinate (HisX)-(His18)Fe(II)cyt$_u$ *c*.

The changes in absorbance associated with the slower process are consistent with conversion of five-coordinate, high-spin (His18)Fe(II)cyt$_u$ *c* to six-coordinate, low-spin (Met80)(His18)Fe(II)cyt$_f$ *c*. Thus, the rate of intramolecular methionine binding to Fe(II)cyt *c* is 16 ± 5 s^{-1} at pH 5, 3.2 M GuHCl. The rate of this step contrasts sharply with the rapid Met binding ($k \sim 2.5 \times 10^4$ s^{-1}) when folding is initiated by CO photolysis in unfolded carbonmonoxy ferrocytochrome *c* (*8*). The difference in Met80 binding rates is likely due to differences in the unfolded proteins. The initial state for ET-triggered folding is (H_2O)(His18)Fe(III)-cyt$_u$ *c*; for folding initiated by CO dissociation, (CO)(His18)-Fe(II)cyt$_u$ *c* is the starting point. The positive charge on the heme in Fe(III)cyt *c* destabilizes the folded protein more than the CO binding in (CO)(His18)Fe(II)cyt *c* (*8*, *9*), and it is likely that the structures of the unfolded forms differ as well.

Kinetics Model. A three-state kinetics model accounts for our results:

$$(\mathrm{His})_2\mathrm{Fe(II)cyt}\ c \underset{k_{+\mathrm{His}}}{\overset{k_{-\mathrm{His}}}{\rightleftharpoons}} (\mathrm{His})\mathrm{Fe(II)cyt}\ c \xrightarrow{k_{+\mathrm{Met}}} (\mathrm{His})(\mathrm{Met})\mathrm{Fe(II)cyt}\ c$$

The general solution to the rate law for this model predicts biphasic kinetics. However, above pH 5.5, ferrocytochrome *c* folding is slow and monophasic ($k_{obsd} = 1-20$ s^{-1}; [GuHCl] = 3.1−4.8 M). Since we observe only (HisX)(His18)Fe(II)-cyt$_u$ *c* and (Met80)(His18)Fe(II)cyt$_f$ *c*, we can invoke the steady-state approximation for the concentration of (His18)-Fe(II)cyt *c*. In this limit, the kinetics will be exponential with an observed rate constant given by

$$k_{obsd} = \frac{k_{-\mathrm{His}}k_{+\mathrm{Met}}}{k_{+\mathrm{His}} + k_{+\mathrm{Met}}}$$

At high pH, folding is limited either by Met80 binding ($k_{+His} \gg k_{+Met}$; $k_{obsd} \sim K_{His}k_{+Met}$, $K_{His} = k_{-His}/k_{+His}$) or by HisX dissociation ($k_{+Met} \gg k_{+His}$; $k_{obsd} \sim k_{-His}$). The observed inhibition of Fe(II)cyt *c* folding (as monitored by heme absorbance) is consistent with the kinetics model, because increasing the imidazole concentration effectively increases k_{+His}.

Below pH 5.5, the folding kinetics are biphasic and all three ligation states of the reduced heme are detected. Under these conditions, the steady-state approximation is no longer valid. The faster kinetics phase reflects the equilibration between (HisX)(His18)Fe(II)cyt$_u$ *c* and (His18)Fe(II)cyt$_u$ *c*, with a pH-dependent rate constant given by $k_{+His} + k_{-His}$. The rate for the slower step is pH independent, and represents k_{+Met}. This assignment is confirmed by transient absorption spectroscopy. Since k_{+Met} does not vary substantially with pH, it is likely that k_{-His} limits ferrocytochrome *c* folding above pH 6.

We have found that k_{obsd} ($\sim k_{-His}$) at pH 7 depends on the folding driving force (rather than absolute denaturant concentration); similar folding rates are found for ferrocytochromes *c* from horse and yeast (with just 40% sequence homology) when the folding free energies are the same (*4*, *10*, *27*). The fact that heme ligand substitution rates correlate with the overall folding free energy suggests that in the final step of Fe(II)cyt *c* folding the barrier does not arise solely from replacing an imidazole ligand by thioether on a ferroheme. Further support for this idea comes from the ET-triggered folding of cytochrome b_{562} (cyt b_{562}). The ferriheme of cyt b_{562} is not trapped by misligated His residues in the unfolded protein, and following photochemical electron injection, the low-spin, (His)(Met)-ligated ferroheme forms about 30 times faster than Met80 binding in the folding of Fe(II)cyt *c* (pH 5) at a comparable driving force (*28*). This comparison suggests that the folding energy landscape (*45*−*48*) for cyt *c* is more rugged than that for formation of the four-helix bundle in cyt b_{562} (*27*).

ACKNOWLEDGMENT

We thank Gary Mines and Torbjörn Pascher for assistance with certain experiments and for helpful discussions.

REFERENCES

1. Babul, J., and Stellwagen, E. (1972) *Biochemistry 11*, 1195−1200.
2. Bixler, J., Bakker, G., and McLendon, G. (1992) *J. Am. Chem. Soc. 114*, 6938−6939.
3. Colón, W., Elöve, G. A., Wakem, L. P., Sherman, F., and Roder, H. (1996) *Biochemistry 35*, 5538−5549.
4. Mines, G. A., Pascher, T., Lee, S. C., Winkler, J. R., and Gray, H. B. (1996) *Chem. Biol. 3*, 491−497.
5. Nall, B., and Landers, T. A. (1981) *Biochemistry 20*, 5403−5411.
6. Pierce, M. M., and Nall, B. T. (1997) *Protein Sci. 6*, 618−627.
7. Yeh, S.-R., and Rousseau, D. L. (1998) *Nat. Struct. Biol. 5*, 222−227.
8. Jones, C. M., Henry, E. R., Hu, Y., Chan, C.-K., Luck, S. D., Bhuyan, A., Roder, H., Hofrichter, J., and Eaton, W. A. (1993) *Proc. Natl. Acad. Sci. U.S.A. 90*, 11860−11864.

9. Pascher, T., Chesick, J. P., Winkler, J. R., and Gray, H. B. (1996) *Science 271*, 1558−560.
10. Mines, G. A., Winkler, J. R., and Gray, H. B. (1998) in *Spectroscopic Methods in Bioinorganic Chemistry* (Solomon, E. I., and Hodgson, K. O., Eds.) pp 198−211, American Chemical Society, Washington, DC.
11. Bushnell, G. W., Louie, G. V., and Brayer, G. D. (1990) *J. Mol. Biol. 214*, 585−595.
12. Tsong, T. Y. (1974) *J. Biol. Chem. 249*, 1988−1990.
13. Hamada, D., Kuroda, Y., Katoaka, M., Aimoto, S., Yoshimura, T., and Goto, Y. (1996) *J. Mol. Biol. 256*, 172−186.
14. Segel, D. J., Fink, A. L., Hodgson, K. O., and Doniach, S. (1998) *Biochemistry 37*, 12443−12451.
15. Colón, W., Wakem, L. P., Sherman, F., and Roder, H. (1997) *Biochemistry 36*, 12535−12541.
16. Bai, Y., Sosnick, T. R., Mayne, L., and Englander, S. W. (1995) *Science 269*, 192−197.
17. Chan, C.-K., Hu, Y., Takahashi, S., Rousseau, D. L., Eaton, W. A., and Hofrichter, J. (1997) *Proc. Natl. Acad. Sci. U.S.A. 94*, 1779−1784.
18. Sosnick, T. R., Mayne, L., and Englander, S. W. (1996) *Proteins: Struct., Funct., Genet. 24*, 413−426.
19. Sosnick, T. R., Shtilerman, M. D., Mayne, L., and Englander, S. W. (1997) *Proc. Natl. Acad. Sci. U.S.A. 94*, 8845−8550.
20. Brems, D. N., and Stellwagen, E. (1983) *J. Biol. Chem. 258*, 3655−3660.
21. Yeh, S.-R., Takahashi, S., Fan, B., and Rousseau, D. L. (1997) *Nat. Struct. Biol. 4*, 51−56.
22. Elöve, G. A., Bhuyan, A. K., and Roder, H. (1994) *Biochemistry 33*, 6925−6935.
23. Shastry, M. C. R., and Roder, H. (1998) *Nat. Struct. Biol. 5*, 385−392.
24. Hagen, S. J., Hofrichter, J., Szabo, A., and Eaton, W. (1996) *Proc. Natl. Acad. Sci. U.S.A. 93*, 11615−11617.
25. Hagen, S. J., Hofrichter, J., and Eaton, W. A. (1997) *J. Phys. Chem. 101*, 2352−2365.
26. Sosnick, T. R., Mayne, L., Hiller, R., and Englander, S. W. (1994) *Nat. Struct. Biol. 1*, 149−156.
27. Telford, J. R., Wittung-Stafshede, P., and Gray, H. B. (1998) *Acc. Chem. Res. 31*, 755−763.
28. Wittung-Stafshede, P., Gray, H. B., and Winkler, J. R. (1997) *J. Am. Chem. Soc. 119*, 9562−9563.
29. Wittung-Stafshede, P., Malmström, B. G., Winkler, J. R., and Gray, H. B. (1998) *J. Phys. Chem. A 102*, 5599−5601.
30. Lindquist, L., Czochralska, B., and Grigorov, I. (1985) *Chem. Phys. Lett. 119*, 494−498.
31. Orii, Y. (1993) *Biochemistry 32*, 11910−11914.
32. Pace, N. C., Shirley, B. A., and Thomson, J. A. (1990) in *Protein Structure: A Practical Approach* (Creighton, T. F., Ed.) pp 311−330, IRL Press, Oxford, England.
33. Wang, J.-S., and Van Wart, H. E. (1989) *J. Phys. Chem. 93*, 7925−7931.
34. Wang, J.-S., Tsai, A. L., Heldt, J., Palmer, G., and Van Wart, H. E. (1992) *J. Biol. Chem. 267*, 15310−15318.
35. Carraway, A. D., McCollum, M. G., and Peterson, J. (1996) *Inorg. Chem. 35*, 6885−6891.
36. Stowell, M. H. B., Larsen, R. W., Winkler, J. R., Rees, D. C., and Chan, S. I. (1993) *J. Phys. Chem. 97*, 3054−3057.
37. Baldwin, D. A., Marques, H. M., and Pratt, J. M. (1986) *J. Inorg. Biochem. 27*, 245−254.
38. Tezcan, F. A., Winkler, J. R., and Gray, H. B. (1998) *J. Am. Chem. Soc. 120*, 13383−13388.
39. Lu, Y., Casimiro, D. R., Bren, K. L., Richards, J. H., and Gray, H. B. (1993) *Proc. Natl. Acad. Sci. U.S.A. 90*, 11456−11459.
40. Bren, K. L., and Gray, H. B. (1993) *J. Am. Chem. Soc. 115*, 10382−10383.
41. Babul, J., and Stellwagen, E. (1971) *Biopolymers 10*, 2359−2361.
42. Tsong, T. Y. (1975) *Biochemistry 14*, 1542−1547.
43. Adams, P. A., Baldwin, D. A., and Marques, H. M. (1996) in *Cytochrome c*: *A Multidisciplinary Approach* (Scott, R. A., and Mauk, A. G., Eds.) pp 635−692, University Science Books, Sausalito, CA.
44. Shao, W. P., Sun, H. Z., Yao, Y. M., and Tang, W. X. (1995) *Inorg. Chem. 34*, 680−687.
45. Bryngelson, J. D., Onuchic, J. N., and Wolynes, P. G. (1995) *Proteins: Struct., Funct., Genet. 21*, 167−195.
46. Socci, N. D., Onuchic, J. N., and Wolynes, P. G. (1996) *J. Chem. Phys. 104*, 5860−5868.
47. Onuchic, J. N., Wolynes, P. G., Luthey-Schulten, Z., and Socci, N. D. (1995) *Proc. Natl. Acad. Sci. U.S.A. 92*, 3626−3630.
48. Wolynes, P. G. (1996) *Proc. Natl. Acad. Sci. U.S.A. 93*, 14249−14255.

BI981933Z